



ELSEVIER

Contents lists available at ScienceDirect

# Superlattices and Microstructures

journal homepage: [www.elsevier.com/locate/superlattices](http://www.elsevier.com/locate/superlattices)

## Effect of gamma-ray irradiation on the device process-induced defects in 4H-SiC epilayers



T. Miyazaki <sup>a</sup>, T. Makino <sup>b</sup>, A. Takeyama <sup>b</sup>, S. Onoda <sup>b</sup>, T. Ohshima <sup>b</sup>, Y. Tanaka <sup>c</sup>,  
M. Kandori <sup>c</sup>, T. Yoshie <sup>c</sup>, Y. Hijikata <sup>a,\*</sup>

<sup>a</sup> Saitama University, Sakura-ku, Saitama 338-8570, Japan

<sup>b</sup> Japan Atomic Energy Agency, Takasaki 370-1292, Japan

<sup>c</sup> Sanken Electric, Niiza, Saitama 352-8666, Japan

### ARTICLE INFO

#### Article history:

Received 18 December 2015

Received in revised form 24 February 2016

Accepted 5 March 2016

Available online 9 March 2016

#### Keywords:

4H-SiC

Gamma-ray irradiation

Photoluminescence (PL) imaging

Basal plane dislocation (BPD)

Stacking fault

Deep level transient spectroscopy (DLTS)

### ABSTRACT

We investigated the gamma-ray irradiation effect on 4H-SiC device process-induced defects by photoluminescence (PL) imaging and deep level transient spectroscopy (DLTS). We found that basal plane dislocations (BPDs) that were present before the irradiation were eliminated by gamma-ray irradiation of 1 MGy. The reduction mechanism of BPD was discussed in terms of BPD-threading edge dislocation (TED) transformation and shrinkage of stacking faults. In addition, the entire PL image was gradually darkened with increasing absorbed dose, which is presumably due to the point defects generated by gamma-ray irradiation. We obtained DLTS peaks that could be assigned to complex defects, termed RD series, and found that the peaks increased with absorbed dose.

© 2016 Elsevier Ltd. All rights reserved.

## 1. Introduction

High radiation resistant devices are required for the aerospace and aircraft industry, and for improving the safety of nuclear energy industry. In particular, MGy-class radiation tolerance of these devices is strongly required for the security of nuclear plant [1]. However, the tolerance of conventional Si devices is 10 kGy order at most. Silicon carbide (SiC) is expected as a high radiation hard device material because of its high bonding strength. Actually, SiC power devices with high radiation resistance have been demonstrated [1]. For example, Tanaka *et al.* demonstrated 10 MGy tolerance of 4H-SiC Buried Gate Static Induction Transistors (BGSITs) [2]. Also Akturk *et al.* reported a high radiation resistance of 4H-SiC commercial metal-oxide-semiconductor field-effect-transistors (MOSFETs) [3]. Although these studies indicated the degradation of device electrical characteristics after gamma-ray irradiation, the radiation damage in the used substrate due to the irradiation has not yet been clarified. In this study, we have investigated the impacts of gamma-ray irradiation on the defects aroused by device fabrication processes such as a basal plane dislocation (BPD). A photoluminescence (PL) imaging and deep level transient spectroscopy (DLTS) were performed for visualization or detection of the defects.

\* Corresponding author.

E-mail address: [yasuto@opt.ees.saitama-u.ac.jp](mailto:yasuto@opt.ees.saitama-u.ac.jp) (Y. Hijikata).

## 2. Experimental procedure

For comparison between radiation damage and electrical characteristic of devices, in this study, epilayers including device structures were employed as samples. The samples used for PL imaging were vertical-type *n*-channel MOSFETs fabricated on a 4H-SiC epiwafer ( $N_d = 8 \times 10^{15} \text{ [cm}^{-3}\text{]}$ ,  $4^\circ$  off-angle), provided from Sanken Electric co., Ltd. We intentionally chose the MOSFET die that has a larger number of BPDs than the others. Fig. 1 shows the cross sectional view of the schematized drawing of MOSFET. The width of Al high implanted layer was  $2 \mu\text{m}$ , that of Al implanted ( $N_a = 1 \times 10^{18} \text{ [cm}^{-3}\text{]}$ ) was  $10 \mu\text{m}$ , and that of P implanted layer was  $3.25 \mu\text{m}$ . In order to take PL images, the three electrodes (gate poly-Si film, source Al pad, and drain Ni contact) and insulators ( $\text{SiO}_2$ ) of MOSFETs were removed by chemical solutions and a SiC epilayer including Al implant (*p*-well) and drift layer was left. PL images were recorded using a cooled CCD camera at room temperature. A He-Cd laser with a 325 nm line and 200 mW output was used as an excitation source.

We also investigated deep levels generated by gamma-ray irradiation. MOS capacitors in the test-element-group (TEG) grown on the same 4H-SiC epiwafer as that for PL imaging were used for DLTS measurements. The oxide thickness was 60 nm. The area and capacitance of the MOS capacitors were  $400 \times 800 \mu\text{m}$  and 26.7 pF, respectively. The sample temperature was varied from 200 to 620 K. The reverse bias was at  $-10 \text{ V}$ , the pulse voltage was 0 V, and the pulse duration was 10 ms. Capacitance increments during 0.24 s (time window  $t_1 = 34 \text{ ms}$  and  $t_2 = 274 \text{ ms}$ ) were recorded as DLTS signals. The DLTS measurements were conducted in dark condition (no excitation source).

Gamma-ray irradiation was performed using a  $^{60}\text{Co}$  source at dose rates between 1 and 10 kGy( $\text{SiO}_2$ )/h up to MGy-class in Japan Atomic Energy Agency (JAEA). We repeatedly conducted PL imaging/DLTS measurements and irradiation for the same sample.

## 3. Results and discussion

Fig. 2 shows PL images taken through a long-pass filter of  $>700 \text{ nm}$  at the same area for the 4H-SiC epilayer at the gamma-ray irradiation of 10 kGy (a), 40 kGy (b), and 1 MGy (c). The stripe pattern parallel to the step flow direction and the black dot in the figures are Al implanted area (shown in Fig. 1) and a position specification marker, respectively. In Fig. 2(a) and (b), bright lines were seen, which were probably basal plane dislocations (BPDs) [4]. Since the bright lines were also seen in the non-irradiated sample (not shown here) and were aligned along the ion-implanted pattern, they are device process-induced defects. However, these BPDs disappeared at irradiation of 1 MGy, as shown in Fig. 2(c).

As the gamma-ray irradiation increased, the entire brightness of PL images were gradually decreased like Fig. 2(b) and (c). This phenomenon were observed all optical filters we used ( $387 \pm 11 \text{ nm}$ ,  $438 \pm 12 \text{ nm}$ ,  $>700 \text{ nm}$ ). The reason may be that point defects generated by gamma-ray irradiation and behaved non-radiative recombination centers.

Fig. 3 shows dependence of BPD area and linear densities on absorbed dose. This result indicates that gamma-ray irradiation has an effect for reducing BPDs. Since the average length of BPD is constant with respect to the absorbed dose, the dependence of area and linear densities vary coincidentally. Nagano *et al.* observed threading edge dislocations (TEDs) by performing PL imaging at IR band [5]. However, TED was not detected in our sample, which may be due to a disturbance of TED emission from device structures. The variation of BPDs can be distinguished into three patterns, i.e. ‘move perpendicular to step flow’ ‘disappear/appear’ and ‘shrink/stretch’.

In general, BPDs consist of perfect dislocation or partial dislocation. Fig. 4 shows PL images taken through a long-pass filter ( $>700 \text{ nm}$ ) and a band-pass filter ( $438 \pm 12 \text{ nm}$ ) at the same area. The band-pass filter can observe single Shockley stacking faults (1SSFs) and the 1SSF is observed as a bright area [6,7]. In Fig. 4(a) and (b), the bright lines in the IR image correspond to the dark lines in the image at 438 nm range (pointed by white arrows in Fig. 4). Also in Fig. 4(b) and (c), the area surrounded by a dark line is brighter than the others. The bright areas, therefore, are SFs and these BPDs are partial dislocations, which are boundaries between SF and perfect crystal. On the other hand, the BPD in Fig. 2 pointed by the white arrow did not include SF. Therefore, this BPD is probably not a partial dislocation but a perfect dislocation.

Here, the reason for BPD elimination due to gamma-ray irradiation will be discussed. In a 4H-SiC substrate, a BPD of perfect dislocation-type and TED easily transform from each other [8]. Looking at the BPD carefully, pointed by the white arrow in Fig. 2(a) and (b), the position of the end at bulk-side (left edge) does not move, whereas the end at the step flow-side (right edge) moves. Therefore, it can be considered that the BPDs are eliminated by transformation from BPD to TED, as illustrated in Fig. 5. On the other hand, the shrinkage of BPDs of partial dislocation-type (pointed by the white arrows in Fig. 4(a) and (b))

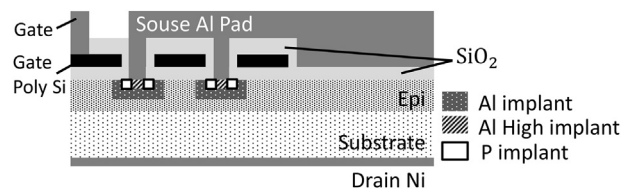


Fig. 1. Schematic drawing of the MOSFET sample for PL imaging.

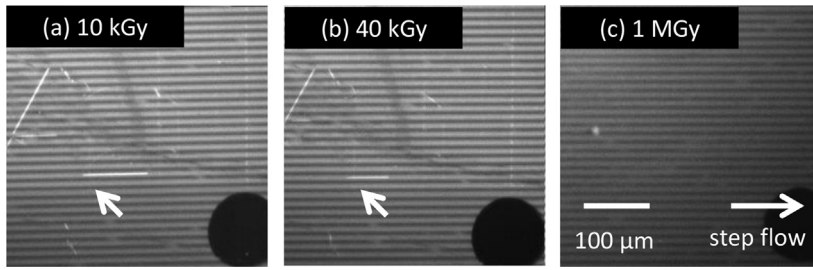


Fig. 2. PL images taken for an irradiated 4H-SiC epilayer through a long-pass filter (>700 nm).

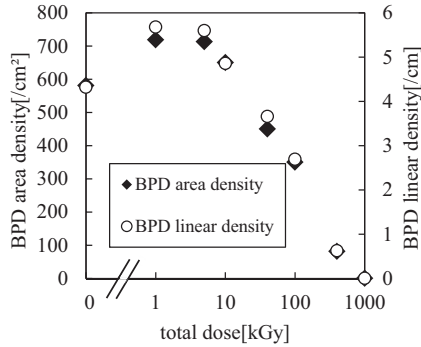


Fig. 3. Dependence of BPD area density and linear density on the gamma-ray absorbed doses.

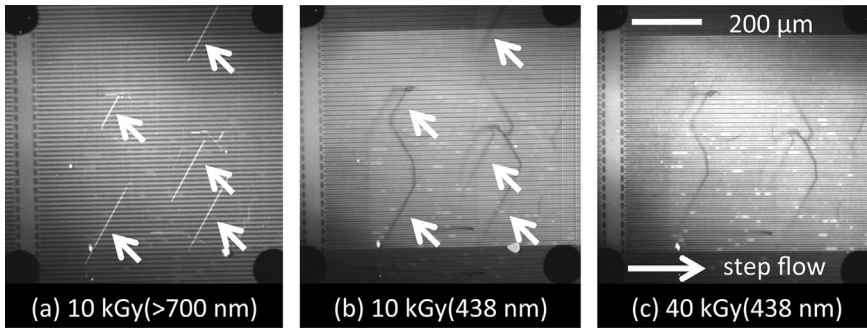


Fig. 4. PL images taken for an irradiated 4H-SiC epilayer through a long-pass filter (>700 nm) at 10 kGy (a), a band-pass filter (438 ± 12 nm) at 10 kGy (b) and at 40 kGy (c).

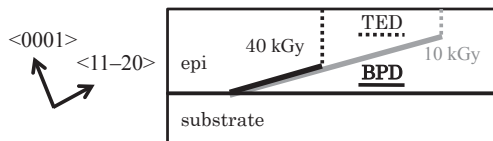


Fig. 5. Cross sectional schematic drawing of the BPD pointed by the white arrow in Fig. 2 (a) and (b). The BPD at around epi/bulk interface (left edge) does not transform but at the surface-side (right edge) transforms to TED due to gamma-ray irradiation.

cannot be explained by this hypothesis. As seen in Fig. 4 (b) and (c), the area of SF is reduced by gamma-ray irradiation. Therefore, the shrinkage or shift of BPD partial dislocation type is probably due to the variation of SF area induced by the irradiation. Miyanagi *et al.* reported that 1SSFs are shrunk by thermal treatment [7]. Thus it is considered that gamma-ray irradiation also has an effect like a thermal treatment.

Fig. 6 shows DLTS spectra at various absorbed doses. Also the peak decomposition of DLTS spectrum at 12 MGy is shown in Fig. 7. As shown in the figure, the DLTS spectrum can be divided into four peaks at 200 K, 390 K, 470 K, and 570 K. We calculated these ionization energies from Arrhenius plots and the values were estimated to be 0.29, 0.83, 1.15, and 1.50 eV

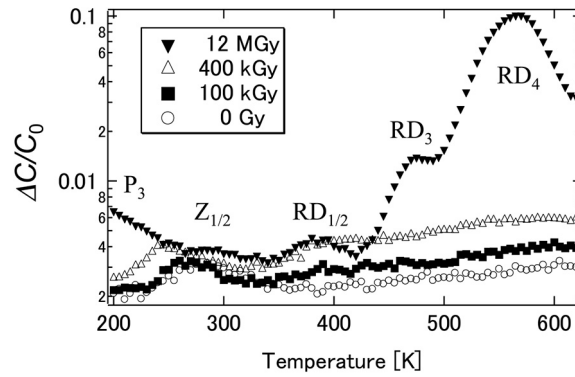


Fig. 6. Absorbed dose dependence of DLTS spectra taken from the *n*-type MOS capacitor fabricated on 4H-SiC epilayer.

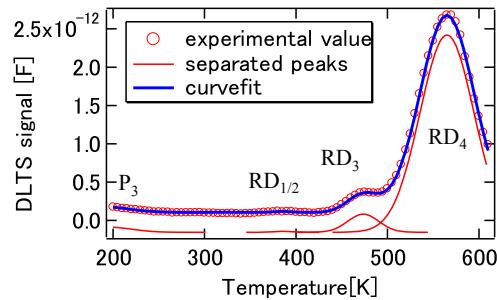


Fig. 7. Decomposition of the DLTS spectrum at 12 MGy.

below the conduction band, respectively. According to previous work [9], the peaks at 390 K (0.83 eV), 470 K (1.15 eV), and 570 K (1.50 eV) can be assigned to RD<sub>1/2</sub>, RD<sub>3</sub>, and RD<sub>4</sub>, respectively. The major deep level for 4H-SiC epilayer, termed Z<sub>1/2</sub> center (300 K, 0.60 eV) originating from carbon vacancy [10], was slightly observed and hardly increased between total doses of 0–400 kGy. Although the peak at 200 K (0.29 eV) was not yet clarified, it may be P<sub>3</sub> [9]. At present, the origins of the RD series peaks are uncertain. Danno *et al.* and Sullivan *et al.* estimated the threshold energy for C and Si displacement as 100 keV [10] and 250 keV [11], respectively. Hence, the internal photoemission generated by gamma-ray irradiation may eject Si and C atoms. However, according to the experimental results, gamma-ray irradiation dose not generate carbon vacancy. In addition, the point defect related to Si is unlikely to form an energy level at the energy range available for *n*-type 4H-SiC [10]. Therefore, the origin of RD series should be complex defects. It has been recently reported that carbon vacancy and Si antisite pairs (V<sub>C</sub>C<sub>Si</sub>) are generated by a high-energy electron irradiation followed by annealing [12–15]. An *ab initio* study performed by Bockstedte *et al.* estimates the ionization energy of V<sub>C</sub>C<sub>Si</sub> as 1.08 eV or 1.45 eV (dependent on charge states) [16], which is almost same as the level of RD<sub>3</sub> and RD<sub>4</sub>. Therefore, the V<sub>C</sub>C<sub>Si</sub> is thought to be one of the candidates for the origin of complex defect.

#### 4. Conclusion

The effect of gamma-ray irradiation on device process-induced defects in 4H-SiC epilayer was investigated by PL imaging. We found that the BPDs were eliminated by gamma-ray irradiation of 1 MGy. The reduction mechanism of BPD was discussed in terms of BPD-TED transformation and shrinkage of stacking fault. The PL images gradually darkened as the increase of absorbed dose, which was thought to be due to point defects generated by gamma-ray irradiation. We also attempted the detection of point defect by performing DLTS and found that gamma-ray irradiation has an effect to generate deep levels, which may be assigned to the RD<sub>1/2</sub> and RD<sub>3</sub> and RD<sub>4</sub>. We regarded the origins of these deep levels as complex point defects such as a V<sub>C</sub>C<sub>Si</sub>.

#### Acknowledgment

This work was partially supported by the Nuclear Science Research Initiative of Japan from Ministry of Education, Culture, Sports, Science, and Technology (MEXT)-Japan (#250402) and Grants-in-Aid for Scientific Research from Japan Society for the Promotion of Science (#15H03967).

## References

- [1] T. Ohshima, S. Onoda, N. Iwamoto, T. Makino, M. Arai, Y. Tanaka, in: Y. Hijikata (Ed.), Chapter 16 of *Physics and Technology of Silicon Carbide Devices*, InTech, Rijeka, 2013, p. 379.
- [2] Y. Tanaka, S. Onoda, A. Takatsuka, T. Ohshima, T. Yasuto, *Mater. Sci. Forum* 941 (2010) 645–648.
- [3] A. Akturk, J.M. McGarrity, S. Potbhare, *IEEE Trans. Nucl. Sci.* 59 (2012) 3258.
- [4] R.E. Stahlbush, K.X. Liu, Q. Zhang, J.J. Sumakeris, *Mater. Sci. Forum* 295 (2007) 556–557.
- [5] M. Nagano, I. Kamata, H. Tsuchida, *Jpn. J. Appl. Phys.* 52 (2013) 04CP09.
- [6] M. Skowronski, S. Ha, *J. Appl. Phys.* 99 (2006) 011101.
- [7] T. Miyanagi, H. Tsuchida, I. Kamata, T. Nakamura, K. Nakayama, R. Ishii, Y. Sugawara, *Appl. Phys. Lett.* 89 (2006) 062104.
- [8] X. Zhang, H. Tsuchida, *J. Appl. Phys.* 111 (2012) 123512.
- [9] T. Dalibor, G. Pensl, H. Matsunami, T. Kimoto, W.J. Choyke, A. Schoner, N. Nordell, *Phys. Stat. Sol. A* 162 (1997) 199.
- [10] K. Danno, T. Kimoto, *J. Appl. Phys.* 100 (2006) 113728.
- [11] W. Sullivan, J.W. Steeds, *Mater. Sci. Forum* 481 (2006) 527–529.
- [12] A.A. Lebedev, A.I. Veinger, D.V. Davydov, *J. Appl. Phys.* 88 (2000) 6265.
- [13] A. Castaldini, A. Cavallini, L. Rigutti, F. Nava, S. Ferrero, F. Giorgis, *J. Appl. Phys.* 98 (2005) 53706.
- [14] G. Izzo, G. Litrico, A. Severino, G. Foti, F. La Via, L. Calcagno, *Mater. Sci. Forum* 615–617 (2009) 397.
- [15] S. Castelletto, B.C. Johnson, V. Ivady, N. Stavrias, T. Umeda, A.Gali, T. Ohshima, *Nat. Mater* 13 (2014) 151.
- [16] M. Bockstedte, A. Mattaus, O. Pankratov, *Phys. Rev. B* 69 (2004) 235202.